Positron annihilation states at SiO_2/Si interfaces: evidence of divacancies

1997 J. Phys.: Condens. Matter 9 10595

(http://iopscience.iop.org/0953-8984/9/48/005)

J. Phys.: Condens. Matter **9** (1997) 10595–10601. Printed in the UK PII: S0953-8984(97)86530-7

Positron annihilation states at SiO_2/Si interfaces: evidence of divacancies

H Kauppinen†, C Corbel†§, L Liszkay†‖, T Laine†, J Oila†, K Saarinen†, P Hautojärvi†, M-F Barthe‡ and G Blondiaux‡

† Laboratory of Physics, Helsinki University of Technology, 02150 Espoo, Finland
‡ Centre d'Etudes et de Recherches par Irradiation, Centre National de la Recherche Scientifique, 3A rue de la Férollerie 45071 Orléans, France

Received 1 August 1997, in final form 3 October 1997

Abstract. We present a method based on positron annihilation to investigate defects at interfaces formed between a thin 10–50 Å overlayer and a substrate. The method applied to 38 SiO_2/Si interfaces gives evidence that (i) high concentrations of divacancies exist in Si domains at the interfaces formed with natural oxides obtained after etching and that (ii) positrons see the same annihilation state at various SiO_2/Si interfaces where the oxides are either commercial, thermally grown, native or obtained after rapid thermal annealing treatments.

Positron annihilation is a powerful method to characterize vacancy-type defects in materials and can be applied to study thin layers as a function of depth by variable-energy positron beams [1]. Whether this method can, however, be developed as a reliable tool to characterize materials at interfaces is still an open question. The main interface studied so far has been the SiO_2/Si interface [2–4] on which the metal oxide semiconductor (MOS) technology relies. Most of the information has been obtained from MOS structures where the thermally grown interfaces are located at 100–500 nm from the SiO_2 surface on which a thin Al layer is deposited. The annihilation characteristics attributed to the SiO_2/Si interface have been found to change under bias [3], hydrogen annealing [5, 6] and vacuum ultraviolet (VUV) irradiation [7] but the origin of the annihilation states occuring at the interfaces is far from understood.

Thin, chemically grown oxides are of increasing interest because many steps in microelectronic technology involve wet-chemical processes in air. As the dimensions of electronic devices decrease and thinner gate oxides are required, the need to understand better the structure and composition of chemically grown interfaces has motivated studies using advanced characterization techniques [8–11]. This paper introduces a novel method of using positron annihilation to characterize the annihilation states at heterointerfaces located at depths of about 10–50 Å. The method is applied to 38 SiO_2/Si interfaces formed in bulk or epitaxial Si materials covered by thin 10–50 Å oxide layers obtained by various processes. Oxides on as-received as well as ion implanted Si have been investigated to determine the intrinsic properties of the interfaces.

§ Permanent address: DRECAM/SCM, Laboratoire CEA de Radiolyse, 91191 Gif sur Yvette, France.
‖ On leave from: Research Institute for Particle and Nuclear Physics, H-1525 Budapest 114, PO Box 49, Hungary.

0953-8984/97/4810595+07$19.50

In this study the positron–electron pair momentum distribution is measured as a function of depth to investigate positron annihilation at the SiO_2 oxide–Si substrate structures [12]. The fraction of annihilations occurring in a low momentum window at the peak, S, and the fraction of annihilations occurring in a high momentum window at the wings, W, are calculated to follow the changes of the momentum distribution. We use both parameters (instead of one as generally used) to define the fingerprint (S_j, W_j) of an annihilation state j. We demonstrate that the annihilation characteristics at the SiO_2/Si interface and in the Si materials can be simultaneously determined by using the S–W plot method introduced earlier for defect investigation in layers or bulk [13–15].

The oxide layers are commercial (×15), thermally grown (×1), native after acid HF etching (120 cm^3 HNO_3, 30 cm^3 CH_3COOH and 12 cm^3 HF) and successive rinsing in deionized water, trichlorethylen and methanol (×21) or result from rapid thermal annealing (RTA) treatments (×3). Oxide thicknesses were determined by nuclear activation analysis of oxygen. The oxide layers are about 10–50 Å thick and cover various Si materials. The samples investigated here are classified in four sets:

(1) *as received* B doped ($p = 2 \times 10^{15}$ cm^{-3}, 10^{15} cm^{-3}, 2×10^{12} cm^{-3}) ⟨100⟩ Czochralski (Cz) (×3), floating zone (×1), and P doped ($n = 1 \times 10^{14}$ cm^{-3}) ⟨111⟩ 90 μm thick chemically vapor deposited (CVD) (×4);

(2) *RTA treated* (Cl vapour lamp, 1200 °C during 5s) in either neutral N_2 (×1) or reductive H_2/Ar atmosphere (×2) B doped ($p = 2 \times 10^{15}$ cm^{-3}) ⟨100⟩ Cz;

(3) *implanted with different ions at various depths and fluences* (Kr/209 MeV 27 μm at different fluences from 5×10^{11} to 1×10^{13} cm^{-2} (×7), BF/210 keV 0.4 μm at fluence 3×10^{13} cm^{-2} (×1), BF_2/343 keV 0.4 μm at fluence 1.5×10^{13} cm^{-2} (×2)) ⟨100⟩ Cz or (H/1.15 MeV 20 μm at fluence 1×10^{14} cm^{-2}) ⟨111⟩ 90 μm thick CVD (×9);

(4) *H implanted and annealed at 400 °C* during 5 min in air ⟨111⟩ 90 μm thick CVD (×8).

The native oxides are formed in the CVD layers which have been etched at various depths from 0 to 25 μm before and after 1.15 MeV H implantation at 300 K, followed by annealing either at 300 or 673 K.

The positron–electron pair momentum distribution was measured at 300 K by recording the Doppler broadening of the 511 keV annihilation line with a Ge detector (FWHM 1.2 keV at 511 keV). Approximately 10^6 events were collected in the peak at each energy value. The window 511[−7.32; +7.32] keV was used to calculate the total number of annihilation events (N_A). The broadening of the annihilation γ-line, ΔE_γ, is proportional to the momentum component of the annihilating electron–positron pair, p_L, along the emission direction of the photons: $2\Delta E_\gamma = cp_L$. Two parameters are used to characterize the shape of the momentum distribution. The low momentum parameter S in the window at the peak, 511[−0.68; +0.68] keV, corresponds to the fraction of annihilations taking place in the momentum range $(0 - |3|) \times 10^{-3} m_0 c$. The high-momentum parameter W in the windows at the wings, 511[−7.32; −2.89] keV and 511[+2.89; +7.32] keV, corresponds to the fraction of annihilations taking place in the momentum range $(|11.3| - |28.7|) \times 10^{-3} m_0 c$.

The energy of the magnetically guided positron beam at the Helsinki University of Technology was changed from 0.1 to 25 keV to vary the positron mean implantation depth in the Si samples from 0.25 nm to 3 μm. The beam energy E was changed in 0.5 keV steps to record the curves $S(E)$ and $W(E)$ [16]. At a given energy, $S(E)$ and $W(E)$ are the averages of the annihilation characteristics in Si, SiO_2 and SiO_2/Si interface weighted by the corresponding annihilation fractions $f_j(E)$. To determine whether only two distinct annihilation characteristics contribute to a set of data (S, W), we use a graphical analysis where we plot S as a function of W [13]. When only two distinct annihilation characteristics

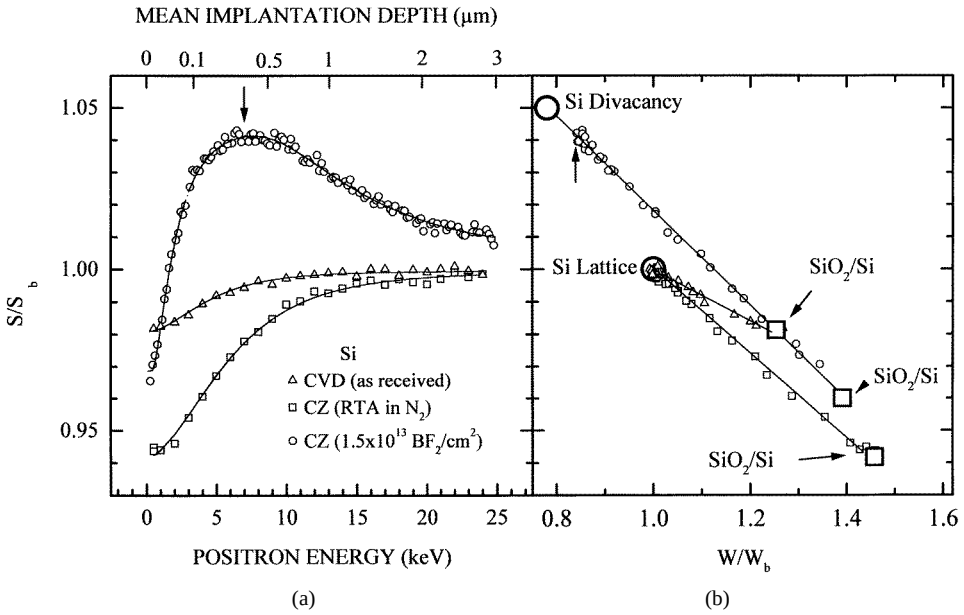

Figure 1. Low momentum fraction $S = N_A([0-|3|]\times 10^{-3}m_0c)/N_A([0-|28.7|]\times 10^{-3}m_0c)$ as a function of positron beam energy (a) and as a function of high momentum fraction $W = N_A([|11.3|-|28.7|]\times 10^{-3}m_0c)/N_A([0-|28.7|]\times 10^{-3}m_0c)$ (b) in various Si materials. The mean implantation depth in Si is $z(E)$ (nm) $= 12.66 \times E^{1.7}$ (keV)[24].

(S_1, W_1) and (S_2, W_2) contribute, the curve $S(W)$ is a segment of a straight line which goes from (S_1, W_1) ($f_1 = 1$) to (S_2, W_2) ($f_2 = 1$). The line is a fingerprint of the superposition of the two annihilation characteristics.

The two lower curves $S(E)$ in figure 1(a) and $S(W)$ in figure 1(b) with the energy E as the running parameter illustrate the typical behaviour found in all the samples except for the BF and BF_2 implanted ones. $S(E)$ increases as energy increases and tends to be constant above 10–15 keV. For $E \geqslant 0.5$ keV, $S(W)$ is a straight line which indicates that positron annihilation can be described with only two annihilation characteristics. One of them characterizes annihilation in the Si substrate at any depth (S_{Si}, W_{Si}) and the other characterizes annihilation at the SiO_2/Si interface (S_{IF}, W_{IF}). They are mixed such that:

$$(S, W) = [\mu_{IF}(E) \times (S_{IF}, W_{IF})] + [(1-\mu_{IF})(E) \times (S_{Si}, W_{Si})].$$

Above 0.5 keV, positrons which diffuse back to the interface are so strongly trapped by the interface that none of them can diffuse through and annihilate in the thin SiO_2 overlayer. The $S(W)$ slope obtained in each sample with the energy E as the running parameter varies strongly from one sample to another, indicating either changes in the Si materials or in the SiO_2/Si interfaces. To determine the two characteristic values in each sample, (S_{Si}, W_{Si}) and (S_{IF}, W_{IF}), with a good statistical accuracy, we fit each experimental $S(W)$ curve to a straight line using a modified version of the VEPFIT [16] program. For each sample, the adjustable parameters in the fitting are the values (S_{Si}, W_{Si}), (S_{IF}, W_{IF}) and the positron diffusion length l^+.

The $S(W)$ straight lines obtained in the samples of the sets (1), (2) and (4) with the energy as the running parameter intersect at the same point. The annihilation signal in the Si material has the same value in all these samples. We assign this value to free positron annihilation in Si lattice $(S_b(Si), W_b(Si)) = (0.5039(1), 0.020\,45(7))$. In

each H and Kr implanted of the set (3), positrons see the damage produced by ion implantation as homogeneous in the Si regions they probed. The Si region probed by positrons corresponds to mean depths of 0–3 μm in the 27 μm Kr implanted samples and of x_e–$x_e + 3$ μm in the samples etched at x_e after the 20 μm H implantation. These regions give different annihilation characteristics depending on the implantation conditions. The $S_{Si}(W_{Si})$ obtained in each of these samples with the energy as running parameter is a straight line which goes through the lattice and the divacancy characteristics that we determined earlier by combining positron lifetime and Doppler broadening experiments in 300 K H implanted Si: $(S_{V_2}(\mathrm{Si}), W_{V_2}(\mathrm{Si})) = (1.050(4) \times S_b(\mathrm{Si}), 0.78(2) \times W_b(\mathrm{Si}))$ with $\tau_{V_2} = 300(4)$ ps $= 1.36(2) \times \tau_b(\mathrm{Si})$ [16]. This indicates that annihilation in implanted Si is a superposition of annihilations in Si lattice and at Si divacancies. It can be further concluded that (i) the dominant defects introduced by the various ion implantation are divacancies and that (ii) only the divacancy concentrations vary from a H or Kr implanted sample to another.

Similar results are obtained for the 0.4 μm BF and BF_2 implanted samples and the latter are shown in figure 1. The curve $S(E)$ corresponding to the BF_2 in figure 1(a) goes through a maximum as the positron energy increases. The maximum is located around 7–8 keV. The curve $S(W)$ (figure 1(b)) is a straight line from 0.5 keV up to only 7 keV. In this energy range, positron annihilation results from the mixing of only two annihilation characteristics, one due to implanted Si and the other to the SiO_2/Si interface. Note that this straight line goes through the Si divacancy point. It follows that in the depth range corresponding to 0.5–7 keV, positrons in implanted Si are totally trapped by Si divacancies at which they annihilate. Above 7 keV, the data deviate from a straight line indicating that, at depth beyond 0.346 μm, the 0.4 μm BF or BF_2 implanted Si materials give rise to the lattice signal in addition to the divacancy one.

The fitted (S_{IF}, W_{IF}) values at the different SiO_2/Si interfaces, vary from $(0.99 \times S_b, 1.15 \times W_b)$ to $(0.93 \times S_b, 1.64 \times W_b)$ indicating that several annihilation states are available at the interfaces. Figure 2 remarkably shows that two straight lines are obtained when the values S_{IF} are plotted as a function of the value W_{IF}. The other noticeable property is that one line goes through the Si divacancy whereas the other goes through the Si lattice. The line on which an interface falls, is independent of the Fermi level, doping and defect concentration in Si. The lack of correlation between the properties of the Si materials and the annihilation characteristics at the SiO_2/Si interfaces suggests that the lines in figure 2 reflect intrinsic properties of the SiO_2/Si interfaces. The point $(S((SiO_2/Si)_{if}), W((SiO_2/Si)_{if}) = (0.898(5) \times S_b(\mathrm{Si}), 1.81(3) \times W_b(\mathrm{Si}))$ where the two straight lines intersect appears as an annihilation signal *common to all interfaces* suggesting that it arises from an interface state, $(SiO_2/Si)_{if}$.

The line from the Si divacancy to the $(SiO_2/Si)_{if}$ interface state characterizes a *first type of interface, IF_1,* which is observed here mainly in the Si materials covered with native or commercial oxides. For this *IF_1 interface,* we propose that positrons annihilate either at Si divacancies or at the $(SiO_2/Si)_{if}$ interface state. The line from the Si lattice to the $(SiO_2/Si)_{if}$ interface state characterizes a *second type of interface, IF_2*. It is observed here in oxides, either thermally grown or obtained after RTA in H_2/Ar or N_2 atmosphere. For this *IF_2 interface,* we propose that positrons annihilate either at Si lattice or at the $(SiO_2/Si)_{if}$ interface states. For each interface, the fractions of annihilation taking place in Si and at the $(SiO_2/Si)_{if}$ interface state are determined from the values S_{IF} (or W_{IF}) at the interface by $f_{IF}(\mathrm{Si}) = 1 - f_{IF}((SiO_2/Si)_{if}) = [S_{IF} - S((SiO_2/Si)_{if})]/[S((Si)_{if}) - S((SiO_2/Si)_{if})]$ where $S((Si)_{if})$ is the Si divacancy for an *IF_1 interface* and the Si lattice for an *IF_2 interface*. The fraction in Si varies from about 20 to 70% for the 34 commercial or native interfaces studied here and from about 25 to 35% in the three RTA and the thermally grown interfaces.

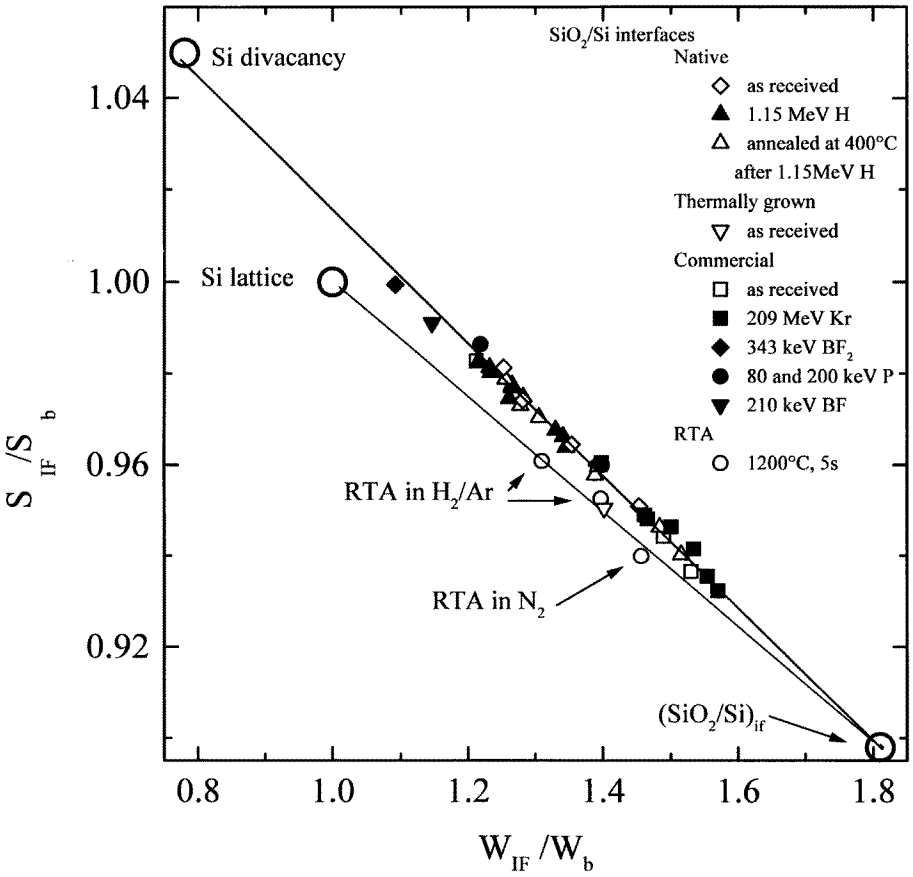

Figure 2. Annihilation characteristics at the SiO_2/Si interfaces in various Si materials: low-momentum fraction S_{IF} as function of the high-momentum fraction W_{IF}. The full straight line joining the Si divacancy and $(SiO_2/Si)_{if}$ interface state is obtained by fitting two sets of data: (1) the (S_{IF}, W_{IF}) data at the interfaces formed with commercial or native oxides obtained after HF etching and (2) the (S, W) data from figure 1(b) in the BF_2 implanted crystal in the energy range 0.5–7 keV. The slope of this line is given by $(W_b/S_b) \times R_{if-V_2} = 0.15 \pm 0.01$ or $R_{if-V_2} = 3.6 \pm 0.1$. The full straight line joining the Si lattice and $(SiO_2/Si)_{if}$ states is obtained by fitting the (S, W) data in the RTA or oxide thermally grown Si in the energy range 0.5–25 keV. The slope of this line is given by $(W_b/S_b)R_{b-if} = 0.124 \pm 0.04$ or $R_{b-if} = 3.0 \pm 0.2$.

In earlier studies, it has been found that buried interfaces formed with thermally grown thick (100–500 nm) oxides give arise to S_{IF}/S_b values ranging from 0.95 to 1.00 depending on oxide growth conditions, thermal annealing, hydrogen passivation etc [3, 7, 18]. It has also been concluded that the interface may have different annihilation sites like open-volume defects and dangling Si bonds (P_b centres) acting as traps for holes and positrons [3]. The reported S_{IF}-values are comparable with those we find here. However, the direct comparison of the $S((SiO_2/Si)_{if})$ interface annihilation state we have identified here as $(0.898(5) \times S_b(Si), 1.81(3) \times W_b(Si))$ is only possible for one study [6] where W values have also been reported. By analysing in the same way as here, the (S, W) data obtained in this study for interfaces in MOS structures under applied bias [6] we can show that these data are consistent with the present SiO_2/Si interface signal we detect here. This seems to

be consistent with the evidence given by x-ray photoelectron spectroscopy that suboxides which are similar to those found in thin chemically grown oxides exist in thin layers of 3–7 Å between the crystalline Si substrate and the thermally grown stoichiometric amorphous SiO_2 [9, 19–21]. It also suggests that the strong positron trapping at the interface may be due to the existence of the suboxide regions.

The probability that positrons near the interface region can escape the $(SiO_2/Si)_{if}$ interface state and annihilate either from Si lattice or Si divacancies is likely to be related to the quality of the interface. At interfaces of good quality, a fraction of positrons diffusing to the interface from the Si material are reflected back and annihilate in Si lattice near the interface. At interfaces of low quality, positrons are partially trapped in Si domains containing high ($> 10^{18}$ cm^{-3}) divacancy concentrations. In this case, one can simply assume that the fraction of positrons trapped at divacancies is proportionnal to the relative areas of the Si domains across the interfaces. Under this assumption we find that the relative area of the Si domains at the SiO_2/Si interface vary from about 20 to 70% in the commercial or native interfaces studied here. The structure of chemically grown $SiO_2/Si(111)$ or $SiO_2/Si(100)$ interfaces has been studied with various other techniques [9], such as infrared spectroscopy (IR), electron energy loss spectroscopy (EELS), scanning transmission microscopy (STM) and atomic force microscopy (AFM) [9, 10, 22]. Interestingly, studies combining IR and STM have shown that after acid HF etching [22] the interface is quite rough and that etching in dilute HF [9, 23] of Si(111) surfaces can lead to the existence of Si domains of $\sim \pi/4 \times$ (10–20 Å)^2 in sections and 3 Å in height accounting for about 50% of the surface. Furthermore the above results show that RTA treatments of 5s at 1200 °C are sufficient to prevent positrons from detecting divacancies either due to the divacancy annealing or hydrogen passivation.

Finally we focus on the electrical fields created by the charge localized at the interfaces. In the samples where positrons in the Si substrate annihilate from lattice, we can infer the charge of the SiO_2/Si interface from the positron diffusion length $l^+(Si)$ in the Si substrate. In the set (1) and (2) of as received and RTA treated samples, the effective diffusion length varies from 63 to 355 nm and can be compared with the free positron diffusion length in Si lattice when there is no field effect, $l_b^+(Si) = 220$–240 nm [25]. The comparison of $l^+(n)$ in the sample n with the positron diffusion length in Si lattice indicates whether the interface charge is negative ($l^+(n) > l_b^+(Si)$) or positive ($l^+(n) < l_b^+(Si)$). In this study, the commercial and native interfaces appear randomly to be slightly positive ($l^+ = 140$ nm) to heavily negative ($l^+ = 355$ nm). The RTA N_2 interface with 290 nm is only slightly negative as found for some interfaces before RTA treatments. In contrast, the RTA H_2/Ar interfaces with 63 and 75 nm appears to be strongly positive. These striking results indicate the reproducible formation of a highly positive interface after RTA treatment in H_2/Ar atmosphere and consequently suggest that very stable donor states are induced at the interfaces by such a treatment.

In summary, in this paper we demonstrate that annihilation characteristics at shallow (10–50 Å) interfaces can be accurately determined when the material below the interface is homogeneous. The interface characteristics (S_{IF}, W_{IF}) are determined from the $S(W)$ straight lines obtained with the positron energy as the running parameter. Furthermore, we show that the intrinsic properties of the interfaces can be investigated by plotting the values $S_{IF}(W_{IF})$ obtained with the interfaces as the running parameter. We illustrate the method with thin SiO_2/Si interfaces and show that native interfaces contain Si divacancies. The method used here can easily be extended to other types of thin interfaces and it opens a new field of investigation to positron annihilation.

Acknowledgments

The authors acknowledge J-L Leray from CEA-EIM and J-L Pelloie from CEA-LETI for kindly supplying a thermally grown sample and E Kotai and K Havancsak from the Research Institute for Particle and Nuclear Physics, Budapest, Hungary for supplying the Kr and BF implanted samples.

References

[1] 1995 *Positron Spectroscopy of Solids* ed A Dupasquier and A P Mills Jr (Amsterdam: IOS)
[2] Peng J P, Lynn K G, Asoka-Kumar P, Becker D P and Harshman D R 1996 *Phys. Rev. Lett.* **76** 2157–60
[3] Asoka-Kumar P, Lynn K G and Welch D O 1994 *J. Appl. Phys.* **76** 4935–82
[4] Anwand W, Brauer G, Coleman P G, Goodyear A, Reuther H and Maser K 1997 *J. Phys.: Condens. Matter* **9** 2947–54
[5] Asoka-Kumar P, Lynn K G, Leung T C, Nielsen B, Rubloff G W and Weinberg Z A 1991 *Phys. Rev.* B **44** 5885
[6] Khatri R, Asoka-Kumar P, Nielsen B, Roellig L O and Lynn K G 1994 *Appl. Phys. Lett.* **65** 330
[7] Clément M, de Nijs J M M, Van Veen A, Schut H and Balk P 1995 *EEE Trans. Nucl. Sci.* **42** 1717
[8] Becker R S, Higashi C S, Chabal Y J and Becker A J 1990 *Phys. Rev. Lett.* **65** 1917
[9] Higashi C S and Chabal Y J 1993 *Handbook of Semiconductor Wafer Cleaning Technology* ed W Kerner (Noyes) pp 433–96
[10] Pietsch G J 1995 *Appl. Phys.* A **60** 347–63
[11] Miura T, Niwano M, Shoji D and Miyamoto N 1996 *J. Appl. Phys.* **79** 4373–80
[12] Hautojärvi P and Corbel C 1995 *Positron Spectroscopy of Solids* ed A Dupasquier and A P Mills Jr (Amsterdam: IOS) pp 491–533
[13] Liszkay L, Corbel C, Baroux L, Hautojärvi P, Bayhan M, Brinkman A W and Tatarenko S 1994 *Appl. Phys. Lett.* **64** 1380
[14] Clement M, de Nijs J M M, Balk P, Schut H and van Veen A 1997 *J. Appl. Phys.* **81** 1943–55
[15] Saarinen K, Laine T, Skog K, Mäkinen J, Hautojärvi P, Rakennus K, Uusimaa P, Salokave A and Pessa M 1996 *Phys. Rev. Lett.* **77** 3407
[16] Kauppinen H, Corbel C, Skog K, Saarinen K, Laine T, Hautojärvi P, Desgardin P and Ntsoenzok E 1997 *Phys. Rev.* B **55** 9598
[17] van Veen A, Schut H, de Vries J, Hakvoort R A and Ijpma M R 1990 *Positron Beams for Solids and Surfaces* ed P J Schultz, G R Massoumi and P J Simpson (New York: AIP) p 171
[18] Leung T C, Asoka-Kumar P, Nielsen B and Lynn K G 1993 *J. Appl. Phys.* **73** 168–84
[19] Grunthaner F J and Maserjian J 1977 *IEEE Trans. Nucl. Sci.* **NS-24** 210
[20] Ogawa H, Terada N, Sugiyama K, Moriki K, Miyata N, Aoyama T, Sugino R, Ito T and Hattori T 1992 *Appl. Surf. Sci.* **56–58** 836
[21] Sugiyama K, Igarashi T, Moriki K, Nagasawa Y, Aoyama T, Sugino R, Ito T and Hattori T 1990 *Japan. J. Appl. Phys.* **29** L2401
[22] Jakob P and Chabal Y J 1991 *J. Chem. Phys.* **95** 2897
[23] Higashi G S, Becker R S, Chabal Y J and Becker A J 1991 *Appl. Phys. Lett.* **58** 165
[24] Soininen E, Mäkinen J, Beyer D and Hautojärvi P 1992 *Phys. Rev.* B **46** 13 104
[25] Mäkinen J, Corbel C, Hautojärvi P, Vehanen A and Mathiot D 1990 *Phys. Rev.* B **42** 1750–8